International Journal of Heat and Technology
Vol. 42, No. 6, December, 2024, pp. 1870-1878
Journal homepage: http://iieta.org/journals/ijht

The Effect of Heat Treatment (T62) on the Tensile Shearing Test of Explosively Welded Layered Material AA2519-AA1050-Ti6Al4V

Maciej Kotyk*, Łukasz Brych

Mechanical Engineering Department, University of Science and Technology, Bydgoszcz 85-789, Poland

Corresponding Author Email: maciej.kotyk@pbs.edu.pl

https://doi.org/10.18280/ijht.420604

Received: 14 September 2024
Revised: 16 November 2024
Accepted: 29 November 2024
Available online: 31 December 2024

Keywords:
high-energy bonding, ANFO, mechanical properties, strength testing, interface, interlayer, lightweight composite, innovative welding technologies

ABSTRACT

The article presents the results of shear testing during tensile loading of a layered material composed of: AA2519-AA1050-Ti6Al4V, before and after heat treatment. The described material was produced using a high-energy explosive welding method utilizing the detonation of ANFO (mixture of NH_4NO_3 and fuel oil). The research was based on monotonic loading of the material with increasing uniaxial load until separation between the gripping parts of the specimen was achieved. During the analysis of the research results, the obtained curves were compared, and a visual analysis of the obtained fractures was conducted. As a result of the conducted research, a significant impact of heat treatment on the described mechanical characteristics was demonstrated. The average value of maximum shear stresses decreased from 77.6 MPa for untreated specimens to an average of 66.3 MPa for heat-treated specimens. The heat treatment caused a slight but noticeable decrease in the tensile shear strength of the examined material. Fractures of the specimens obtained from the experiment confirm that, in studied cases, separation of individual fragments of specimens exhibited cohesive characteristics within interlayer material, regardless of whether material was heat treated. Results of this work is elimination of main doubts related to explosive welding of materials by indicating location of damage in technical objects. As demonstrated by the conducted research, in the case of the presented material, potential local post-weld delamination will not have a critical impact on the composite's strength. The separation-type damage is most likely to exhibit a cohesive nature within the mechanically weakest material (aluminum alloy 1050).

1. INTRODUCTION

The contemporary demand for advanced engineering materials is substantial. This arises from the desire for continuous development and, also for commercial reasons. It is important not to solely associate this with the demand for materials with ever-increasing strength properties. Significantly, resistance to external factors such as corrosive environments, elevated temperatures, as well as exposure to radiation or ballistic loads, cannot be overlooked. In the context of modern capabilities, it is challenging to find a material that successfully combines even two of these mentioned characteristics in one material. Composite or layered materials serve as alternative solutions. In the case of the latter, their application is associated with the necessity of developing a method for their durable joining. One of the methods allowing for the joining of materials with significantly differing mechanical properties is the high-energy explosive welding method [1].

In the described technology, material joining occurs due to dynamic interactions between materials impacting each other at high velocities. Achieving success with this technology enables the bonding of materials that cannot be joined by more conventional methods, such as welding with an electrode or welding wire. Prospect of utilizing such materials is vast. Such composites are currently employed, among other applications, in aerospace structures are also envisioned for the construction of joints between weldable and non-weldable materials, notably in the shipbuilding industry [2]. Therefore, the use of composite engineering materials produced through explosive welding is justified, provided it is carried out in a deliberate and safe manner.

In addition to their utilitarian merits, a particularly intriguing aspect from both a cognitive and structural standpoint is understanding the mechanical properties of such materials in various environmental conditions. The results of mechanical characterization studies are challenging to interpret, as conventional methods for determining these parameters are known but were not developed for materials (structures) composed of at least two significantly different materials. Furthermore, it should be noted that there exists a bonding layer within the material, where interaction between the materials occurs. The joining process itself also remains significant.

Hence, this article is dedicated to the identification of selected mechanical properties of the bonding layer.

The discussed issue may be noticeable both during tests with monotonically increasing loads as well as during fatigue and cyclic tests. As a result, a common type of damage that can be identified in layered materials is delamination [3, 4]. It

can occur within the material without the possibility of being observed with the naked eye or without use of specialized equipment. Hence, there is particular interest in studying the fracture behavior in such structures. Consequently, it was decided to place special emphasis on investigating the mechanical strength of the bonding layer itself. An example of such an experiment allowing for the determination of the mechanical properties of this area is tensile shear testing, where the sheared layer is the intermediate area between the base materials. Described research on damage characteristics of layered materials was conducted on layered material AA2519-AA1050-Ti6Al4V (Al-Ti) to determine modes of failure for this composite under mechanical impacts focused on bonding layer.

Although the AA2519-AA1050-Ti6Al4V material was recently developed and, at the time of writing this article, was solely for experimental purposes, publications on its topic can be found in the readily available literature on experimental solid mechanics. Some of these publications focus on selected mechanical properties of AA2519-AA1050-Ti6Al4V [5]. Among them, there are studies concerning the strength under monotonically increasing loads [6-8]. Additionally, a study was encountered in which particular emphasis was placed on characterizing the fracture toughness of the described material [9, 10]. None of authored works or articles found in publicly available literature directly addressed mechanical properties of bonding layer.

Similarly, in the case of studies regarding the microstructure and microhardness of this material [11]. In works from this area, it has been demonstrated that intermetallic compounds such as Al_3Ti, occurring among others in the material discussed in this article, lead to their local hardening. This is not always advantageous, as although they enhance the ballistic resistance of such materials, the formation of Al3Ti particles induces discontinuities in the material structure. As a result, point-like, local stress concentrations arise as a consequence of the formation of inclusions [12]. Information about the unfavorable consequences of the occurrence of these discontinuities can be found in readily available sources. The consequence of their presence is the formation of voids within the material. Stress accumulation within these voids increases the likelihood of discontinuities in the material in the form of cracks and delamination [13, 14].

The research was also conducted to determine the fatigue life of the AA2519-AA1050-Ti6Al4V material. In the readily available literature, a cycle of publications dedicated to the described Al-Al-Ti material feature can be found [15-17]. It should be noted that the material presented in the aforementioned three articles represents a different variant of the layered material than that described in this article. The fundamental difference lies in the thickness of the individual layers of the base materials. The differences concerned the buffer layer made of the AA1050 alloy. In the mentioned works, the thickness of the layer made of the AA1050 alloy was approximately 500 μm, while in this article, the thickness of the buffer layer (AA1050) is 1000 μm. It should be remembered that the transitional zone (joining) is geometrically complex, and its thickness cannot be unequivocally determined, and the provided value serves only as an approximate measure. This reinforces belief that strength studies of Al-Ti composite, focused solely on bonding layer strength, are justified.

For materials constructed solely of or including aluminum alloys from the 2XXX [18] series, thermal processing is crucial for achieving high mechanical characteristics and maintaining their mechanical properties in connections that are currently in the experimental phase [19]. In the readily available literature, information regarding the influence of heat treatment on Al-Al-Ti materials can be found [20, 21]. In these works, it was noted that heat treatment is conducted to relieve stresses resulting from the highly rapid process of explosive welding. Thermal homogenization also induces changes in the microstructure of the aluminum alloy [22]. An elevated temperature accelerates chemical reactions, including oxidation. The phenomenon of oxidation is also observed during the thermal homogenization of aluminum alloys. In publicly available sources, studies have been found addressing this topic in the context of layered materials based on Al-Al-Ti materials [23-25]. However, these studies primarily focus on physical changes and the influence of environmental factors on selected properties. Mechanical strength of these materials is not extensively discussed in them. All of this leads to the conviction that heat treatment, necessary to achieve high mechanical properties for AA2519, must also be experimentally verified in terms of shear strength of bonding layer in Al-Ti composite, as it may influence failure mode of this layer.

The articles found in the literature allow for the recognition of the utility of materials based on titanium alloys and aluminum alloys, including AA2519-AA1050-Ti6Al4V. To successfully utilize such materials, it is necessary to identify their mechanical properties, with particular emphasis on the transitional zone between these materials, due to the difficulty of unequivocally determining its mechanical properties. This situation is further complicated by the need for heat treatment. Therefore, it was deemed appropriate to research the mechanical properties of the intermediate layer in the layered material AA2519-AA1050-Ti6Al4V.

2. MATERIALS AND METHODS

2.1 Material

The material investigated in this article constitutes an explosively welded combination of three materials. The first of the base materials is the AA2519 [26, 27] aluminum alloy, the second is the Ti6Al4V titanium alloy (grade 5) [26], while the intermediary material is the AA1050 aluminum alloy.

The chemical compositions of the respective materials are provided in Table 1 for the AA2519 material, in Table 2 for the Ti6Al4V material, and Table 3 for the AA1050 alloy [4]. Figure 1 schematically illustrates the manufacturing and heat treatment process of the Al-Ti layered material, along with a photograph depicting a section of the tested material, including the respective thicknesses of the individual layers, as well as an enlarged view of the intermediate layer.

Table 1. Chemical composition of AA2519 (weight %) [4]

Materials	Si	Fe	Cu	Mg	Zn	Ti	V	Al
Composition	0.06	0.08	5.77	0.18	0.01	0.04	0.12	bal.

Table 2. Chemical composition of AA1050 (weight %) [28, 29]

Materials	Mn	Fe	Si	Mg	Cu	Ti	Zn	Al
Composition	0.05	0,4	0.25	0.05	0.06	0.05	0.07	bal.

Table 3. Chemical composition of Ti6Al4V (weight %) [30]

Materials	Al	V	Fe	Si	O	C	N	Ti
Composition	6.42	4.12	0.18	0.024	0.12	0.013	0.011	bal.

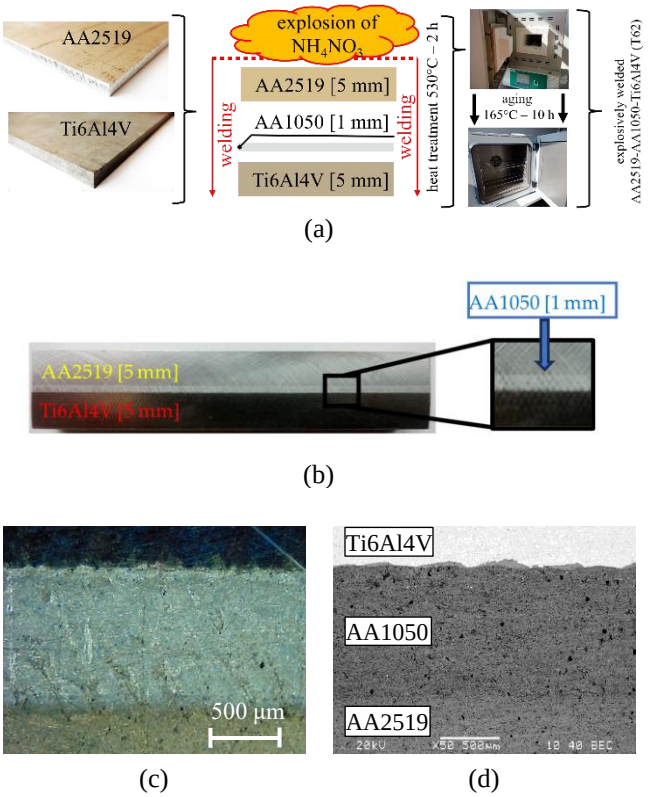

Figure 1. Material specimen piece from which the specimens for testing were prepared, specifying the thickness of each layer: (a) schematic of the manufacturing and heat treatment process of the composite; (b) general view; (c) optical microscope image; (d) SEM view

Experimental material plates of the developed AA2519-AA1050-Ti6Al4V layered material were produced by Explomet. According to the developed technology, the bonding was achieved through parallel cladding of the AA2519 aluminum layer and the Ti6Al4V titanium layer, with the light alloy being the deposited layer. As a result, the titanium did not come into direct contact with the explosion. Before the bonding process, a 1 mm thick layer of AA1050 alloy was rolled onto the aluminum alloy. The welding process was conducted so that the flame front propagation speed during detonation ranged from 1850 m/s to 2000 m/s, with an impact angle of 15°. The result of these procedures is achieving a bonding speed of 420 – 620 mm/s and the formation of a geometrically complex structure in the bonding layer.

2.2 Methods

Six specimens were subjected to tensile shear testing. Three specimens underwent solution heat treatment - two hours at 530°C followed by quenching in water at ambient conditions, and ten hours of artificial aging at 165°C. The remaining three specimens remained in the as-received state. The dimensional cutting of the specimens was outsourced, while the notches were made using an electrical discharge machining (EDM) machine. The dimensions and shape of the tested specimens are depicted in Figure 2, while the EDM machine used for specimen preparation is shown in Figure 3.

It is difficult to precisely determine the direction of sheet bonding. The welding process involves multiple explosion initiators distributed across the entire surface of the sheet. The flame front propagates in all directions. This is visible as circular depressions in the aluminum layer at the points where the explosion initiators were placed. The charges are detonated in a sequence to achieve a directional structure. Due to the significant difficulty in determining this structure, the specimens were cut so that the direction of the applied force would be parallel to the rolling direction of the AA2519 aluminum layer. Notches in the specimens, with a width of 0.32 mm, were made to ensure the generation of shear forces in the joining zone during tension testing. The geometry of the specimens was developed based on the information contained in the ISO 4587:2003 standard [31].

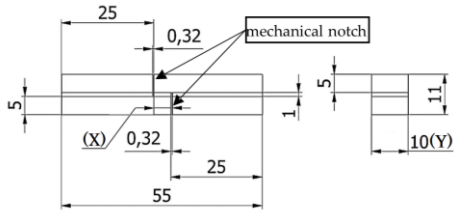

Figure 2. Shape and main dimensions of specimen (dimensions in millimeters)

Figure 3. The equipment used during specimen preparation: (a) wire EDM machine BP 95d; (b) view of the panel with presented parameters for processing the Al-Al-Ti layered material

Figure 4. Measurement setup during the experiments: (a) mechanical testing machine with specimen clamped in the grips; (b) start of the shearing test; (c) end of the experiment

Tensile shear test of Al-Al-Ti specimens was conducted using a dual-column INSTRON 5966 mechanical testing machine. The experiment involved shearing the bonding zone

of the layered material specimen using axial tensile loading. The specimens were placed in the grips of the mechanical testing machine. Subsequently, the shearing test commenced at a constant displacement rate of 0.02 mm per second. The test was conducted until the material specimen's integrity was disrupted. A view of the testing setup and the mounted specimen in the grips of the mechanical testing machine is shown in Figure 4.

Before conducting the shear strength evaluates, measurements of the tested specimens were performed. The geometric dimensions of the bonding zones of the layered material were measured. This measurement allowed for the precise determination of the shear strength of individual specimens. The dimension "x" (see Figure 2) of the discussed area of the bonding zone was measured optically using DLTCamViewer software, while the dimension "y" (see Figure 2) was measured using a standard mechanical micrometer. Each measurement was performed three times. The measurement results were placed in Table 4 as the average of three measurements for each specimen. The average value of each measurement was calculated according to the following formula:

$$\bar{x} = \frac{\sum_{i=1}^{n} x_i}{n} \tag{1}$$

To evaluate the dispersion of results, standard deviation was calculated as a measure of spread of obtained values relative to the mean value, in accordance with the formula:

$$\sigma = \sqrt{\frac{\sum(\tau_i - \bar{\tau}_i)}{N}} \tag{2}$$

Table 4. Designation and average geometric dimensions (mm) of the measurement part of the specimens

Specimen Signature	Width "x"	Thickness "y"
5.12A_TST_01_NOC	4,72	9,92
5.12A_TST_02_NOC	4,67	9,87
5.12A_TST_03_NOC	4,75	9,89
5.12A_TST_01_OC	4,71	9,87
5.12A_TST_02_OC	4,76	9,83
5.12A_TST_03_OC	4,73	9,92

Table 5. Compilation of selected measurement results and research findings

Specimen (without 5.12A_TST)	Maximal Load F (N)	Cross-Sectional Area S (mm^2)	τ, (MPa)	σ Standard Deviation
01_NOC	3627	46.82	77.5	σ_{NOC} 0.49
02_NOC	3609	46.09	78.3	
03_NOC	3621	46.98	77.1	
mean value for NOC	3619	46.63	$\bar{\tau}_{NOC} = 77.6$	
01_OC	3106	46.49	66.8	σ_{OC} 0.51
02_OC	3113	46.79	66.5	
03_OC	3079	46.92	65.6	
mean value for OC	3099	46.73	$\bar{\tau}_{OC} = 66.3$	
Δ%	14.59%			

In the presented equation, the subscript *i* represents a variant of heat treatment (OC or NOC), while *N* is the size of the population. The percentage difference in strength of examined specimens before and after heat treatment (see Table 5) was calculated using a formula:

$$\Delta\% = \left|\frac{\bar{\tau}_{NOC} - \bar{\tau}_{OC}}{\bar{\tau}_{NOC}}\right| \cdot 100\% \tag{3}$$

3. RESULTS AND DISCUSSION

Using the research methodology described in Chapter 2, the shear strength of the explosively welded bonding zone of the AA2519-AA1050-Ti6A14V material was determined in two states: before and after heat treatment. Six specimens were subjected to mechanical loading. Three of them were labeled with the code 5.12A_TST_XX_NOC, where "XX" indicates the specimen number (01, 02, or 03), and "NOC" indicates "not heat-treated." The remaining three specimens were coded as 5.12A_TST_XX_OC, where "XX" again denotes the specimen number (01, 02, or 03), and "OC" indicates "heat-treated."

During the tensile shear testing, the testing machine records the experiment results in from measurement channels. Based on the obtained data, stress-strain curves were prepared, showing the calculated course of the conducted strength tests. To prepare these curves, it was necessary to calculate the registered force into shear stress. To do this, the following relationship was used:

$$P = x \cdot y \tag{4}$$

After calculating areas of cut surfaces of specimens and reading maximum shear force value, shear stresses for each tested specimen were determined according to formula:

$$\tau = \frac{F}{P} \tag{5}$$

After converting the registered force values into shear stresses, graphs were plotted to depict the stress versus the displacement of the testing machine's crosshead. These curves were illustrated in Figure 5 for the virgin specimens and in Figure 6 for the heat-treated specimens. A comparison of all obtained curves is presented in Figure 7. The measurements obtained and selected research results, considered particularly significant for the interpretation of the research findings, have been compiled in Table 5. The results of the maximum shear stress values for all tested specimens are presented graphically in Figure 8.

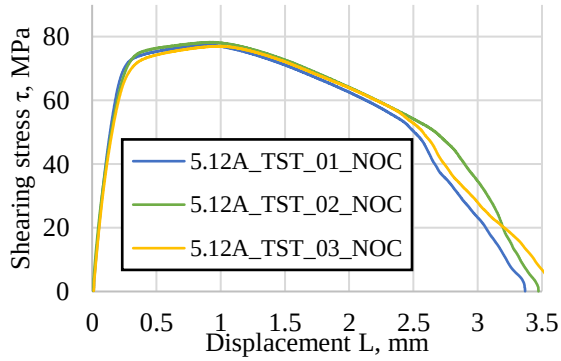

Figure 5. Shear stress-displacement curves plotted for the specimens untreated thermally

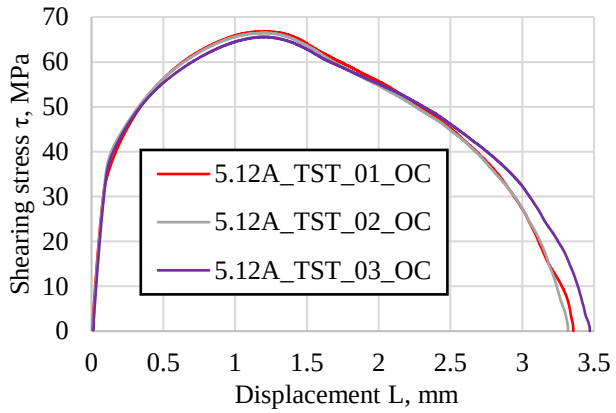

Figure 6. Shear stress-displacement curves determined for thermally treated specimens

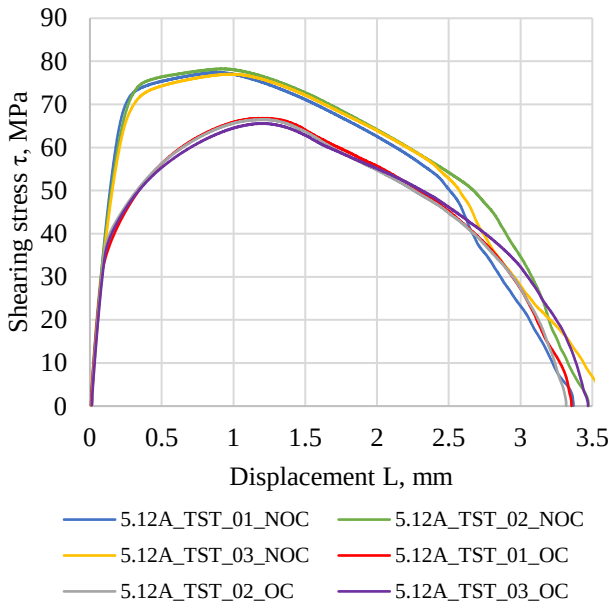

Figure 7. Comparison of all obtained

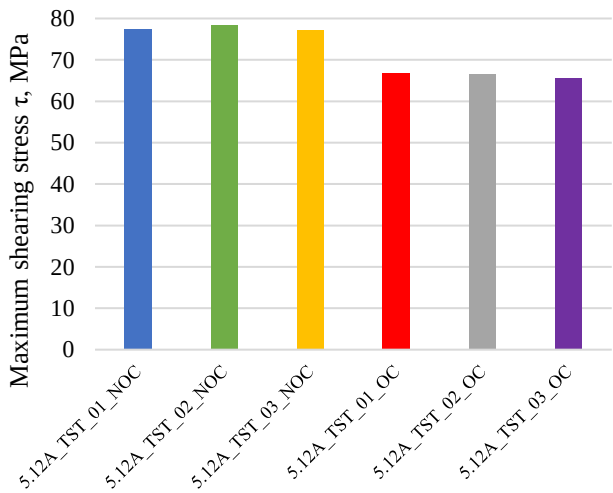

Figure 8. Results of the maximum shear stress values for all tested specimens

After conducting the experiment, fracture surfaces of specimens were obtained. The fracture structure of thermally treated specimens differs from that of non-thermally treated ones. Non-thermally treated specimens exhibit fractures divided into two zones. In the first zone, the direction of loading is visible, while the second zone does not show this directionality. Conversely, for thermally treated specimens, the division of these zones disappears on one side of the fractures. A comparison of the fractures for "NOC" and "OC" specimens is presented in Figure 9.

The lateral view of the specimens shows a triangular-shaped fracture, indicating the occurrence of bending during conducted tensile-shear tests. It is worth noting that the buffer layer in the investigated material exhibits lower mechanical strength compared to other layers. Even a slight bending moment compared to tensile force would contribute to such a fracture. No difference was observed in the lateral view of fractures between non-thermally treated and thermally treated specimens. All specimens have a similar lateral shape. A comparison of lateral views of fractures for selected "NOC" and "OC" specimens is presented in Figure 10. Photographs of all specimens after testing, showing a side view of specimen and the fracture surface, are presented in Figure 11.

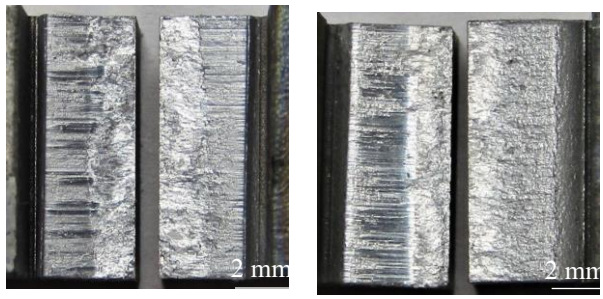

(a) (b)

Figure 9. Comparison of fracture surfaces of selected specimens: (a) 5.12A_TST_01_NOC; (b) 5.12A_TST_01_OC

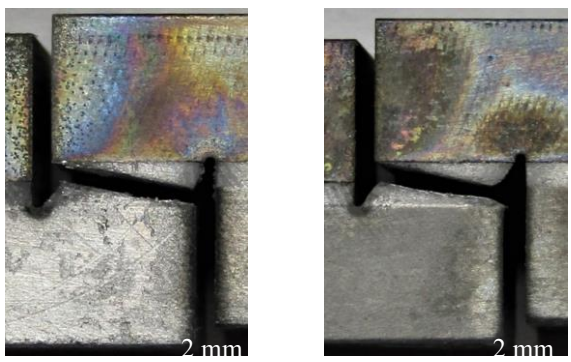

(a) (b)

Figure 10. Comparison of side views of fracture surfaces of specimens: (a) 5.12A_TST_02_NOC; (b) 5.12A_TST_03_OC

Specimen 02 exhibited the highest shear strength among non-heat-treated specimens. Average shear strength for "NOC" specimens is 77.6 MPa. Specimen 01 showed the highest shear strength among heat-treated specimens. Average shear strength for "OC" specimens is 66.3 MPa. Heat-treated specimens generally demonstrated lower shear strength under tension compared to non-heat-treated specimens. This difference amounts to 14.6% in favour of non-heat-treated material. Particular attention should be given to repeatability of results, understood as a small standard deviation from the

arithmetic mean within a single state of heat treatment. In both examined cases, the described variability of results fluctuated around 0.5 MPa, representing less than 1% of the mean value. In relation to studies within mechanical engineering, the obtained results provide strong evidence to consider the experiment properly conducted. A small standard deviation in the case of specimens without heat treatment may also indicate a stable internal state of the intermediate layer made of AA1050 material. However, this could be questionable, as notches on samples perpendicular to the axis might induce release of residual stresses in the composite. Definitive validation of this hypothesis, however, requires additional research.

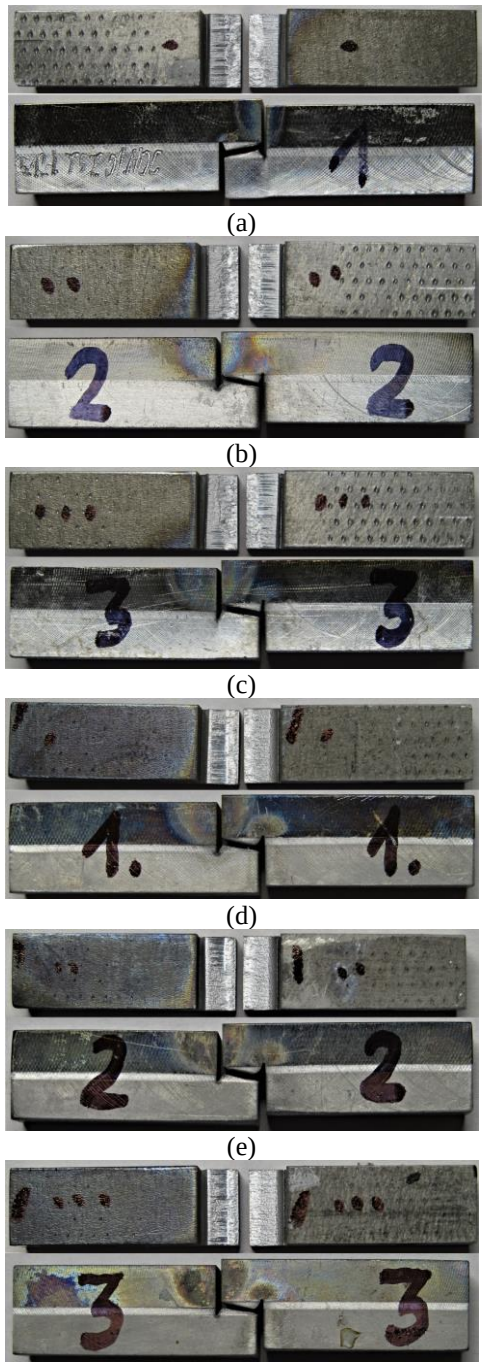

Figure 11. Comparison of side views of fracture surfaces of specimens: (a) 5.12A_TST_02_NOC; (b) 5.12A_TST_03_OC (dimensions are consistent with Figure 2)

Visual analysis of specimens revealed that the fracture mechanism was consistent across all specimens. Fracture occurred exclusively in cohesive manner within AA1050 intermediate material. Influence of bending moment during testing using flat specimens was evident in all specimens. As observed in Illustration 7, initial stiffness of both heat-treated and non-heat-treated specimens was similar. Heat treatment resulted in decrease in joint strength and sharper transition from linear to plastic portion of stress-strain curve. All tested specimens experienced separation at very similar displacements regardless of thermal normalization.

To determine in which area of the composite the fracture occurs and what the impact of heat treatment is on the strength and nature of the fracture for the described Al-Al-Ti layered material, an analysis was conducted on both the specimens themselves and their fracture surfaces using optical microscopes and a scanning electron microscope (SEM). Photographs of the side of a selected specimen with a visible mechanical notch and the immediate vicinity of the initial shear area are presented in Figure 12. SEM photograph showing a macro view of the fracture of a selected non-heat-treated specimen is presented in Figure 13, and a detailed view is shown in Figure 14. Similarly prepared photographs for the heat-treated material are presented in Figures 15 and 16, respectively.

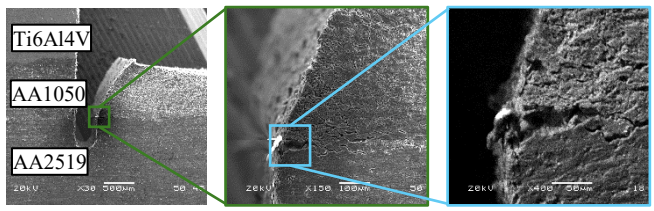

Figure 12. Side view of the specimen showing tip of an adhesive microcrack

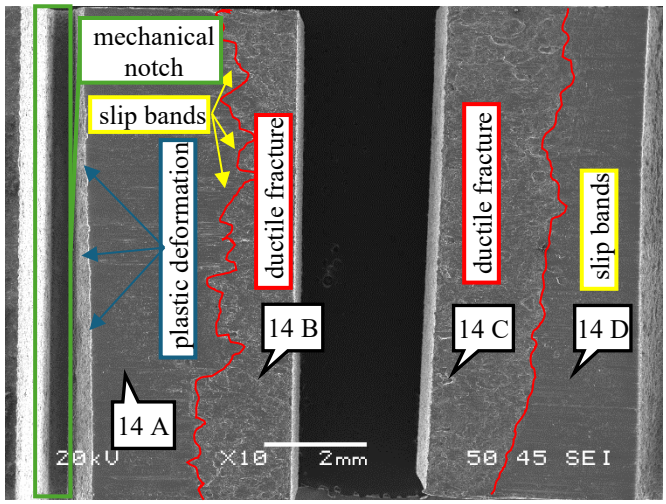

Figure 13. Fracture of the selected not heat-treated specimen intended for TST testing

Figure 12 shows that the tested specimen exhibited significant plastic deformation around mechanical notch and localized cohesive secondary fractures within AA1050 alloy. There is also a small and shallow adhesive crack between AA2519 and AA1050 alloys. However, adhesion strength was sufficiently high that, along the remaining length of the composite, separation occurred exclusively within the

interlayer material, i.e., AA1050 alloy. This provides a strong basis for concluding that bond strength is greater than cohesive strength of weakest material used in construction of composite, namely AA1050 alloy.

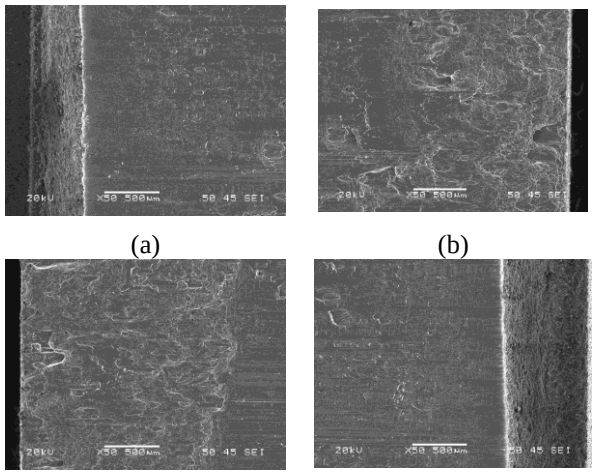

(a) (b) (c) (d)

Figure 14. Selected fracture sections of the non-heat-treated specimen: a) section 14 A; b) section 14 B; c) section 14 C; d) section 14 D, as shown in Figure 13

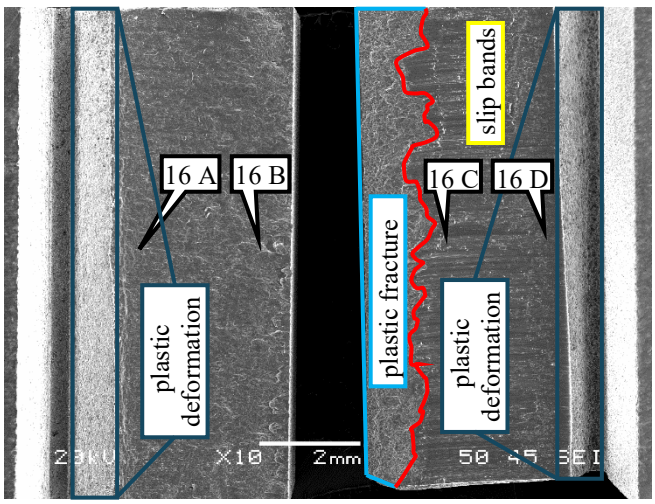

Figure 15. Fracture of the selected heat-treated specimen intended for TST testing

Fractures of both specimens seem to have common features. In both the heat-treated and non-heat-treated specimens, at least 3 very distinct areas can be identified on the fracture. First one is the area of plastic deformation, the second is the area with very distinct slip marks, and third is the area of plastic fracture. On both fractures, the direction of loading can be observed. The main difference between fractures is that zone of plastic deformation (visible on side in Figure 12) is significantly larger in fracture of heat-treated specimen. This most likely indicates that operations at elevated temperatures have increased plasticity of AA1050 alloy.

During a detailed analysis of fractures (at a slightly higher magnification), another difference between fractures was observed. In fracture of non-heat-treated specimen, structures parallel to loading direction with transverse secondary micropores were uniformly present across entire surface. This phenomenon had a global nature but was randomly distributed throughout fracture surface. This may indicate that heat treatment, in addition to changing mechanical properties of buffer layer, also homogenizes structure inside material. Described structure is presented in Figure 17.

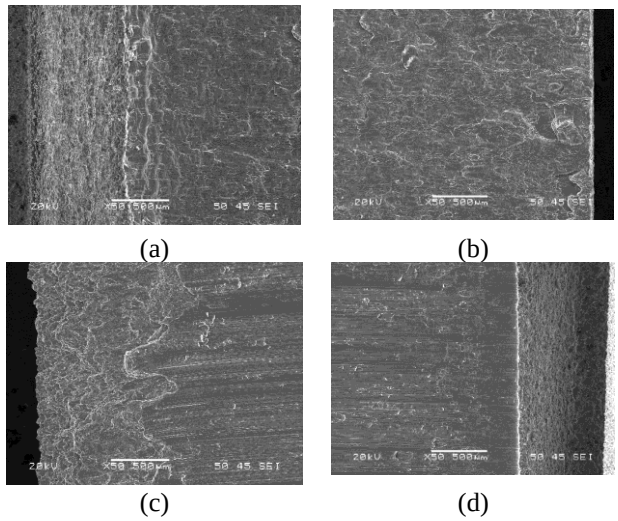

(a) (b) (c) (d)

Figure 16. Selected fracture sections of the heat-treated specimen: a) section 16 A; b) section 16 B; c) section 16 C; d) section 16 D, as shown in Figure 15

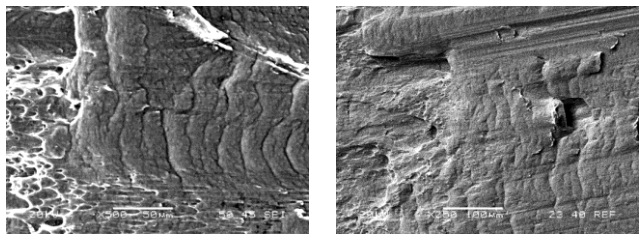

(a) (b)

Figure 17. The structure observed on the fracture of the non-heat-treated specimen: a) secondary electron image view; b) reflective electron image view

As demonstrated during fractographic analysis, despite differences in morphology of fractures, there was no change in overall nature of fracture in which cracking occurs exclusively within buffer material made of AA1050 alloy and not adhesively between layers. It is also important to note that heat treatment itself aims to improve mechanical properties of AA2519 aluminum alloy, which is irrelevant in presented study but affects strength of joint itself without altering way it fractures.

4. CONCLUSIONS

Heat treatment affects the maximum value of shear stress at the interface in AA2519-AA1050-Ti6Al4V layered materials. Considering all tested specimens, it can be inferred that the joint strength is greater than the cohesive strength in the AA1050 material, regardless of whether the material is in the as-delivered state or in the T62 state.

Heat treatment of this material resulted in a reduction of nearly 15% in shear strength under tensile loading for the AA2519-AA1050-Ti6Al4V layered material from an average value of 77.6 MPa for samples not subjected to heat treatment to a value of 66.3 MPa for specimens after heat treatment.

The application of the methodology described in the article in

the studied cases resulted in result repeatability understood as a small standard deviation value fluctuating around 0.5% of the average value in both analysed cases. It may serve as a basis for using this method in determining a selected strength characteristic of explosively welded layered materials.

Local triangular shape observed in the side view of specimen suggests that measuring angle between shorter side of triangle and its base provides the possibility of determining the Kirchhoff modulus. However, it should be noted that after separation, elastic stresses are released, and the value of mentioned modulus, when determined directly, is subject to error.

REFERENCES

[1] Greenberg, B.A., Ivanov, M.A., Kuz'min, S.V., Lysak, V.I. (2020). Explosive Welding Prosesses and Structures. Boca Raton: Taylor & Francis Group. https://doi.org/https://doi.org/10.1201/9780429340550

[2] Boroński, D., Skibicki, A., Maćkowiak, P., Płaczek, D. (2020). Modeling and analysis of thin-walled Al/steel explosion welded transition joints for shipbuilding applications. Marine Structures, 74: 102843. https://doi.org/10.1016/j.marstruc.2020.102843

[3] Boroński, D., Dzioba, I., Kotyk, M., Krampikowska, A., Pala, R. (2020). Investigation of the fracture process of explosively welded AA2519-AA1050-Ti6Al4V layered material. Materials, 13(10): 2226. https://doi.org/10.3390/ma13102226

[4] Kotyk, M. (2020). Analytic model of maximal experimental value of stress intensity factor Kq for AA2519–AA1050–Ti6Al4V layered material. Materials 13(19): 4439. https://doi.org/10.3390/ma13194439

[5] Kotyk, M. (2024). Effect of cryogenic conditions on the critical crack tip opening displacement for the laminated material AA2519-AA1050-Ti6Al4V-T62. Journal of Materials Research and Technology, 28: 3319-3332. https://doi.org/10.1016/j.jmrt.2023.12.211

[6] Najwer, M., Niesłony, P. (2016). Microhardness and strength properties of metallic joint AA2519-AA1050-Ti6Al4V after various heat treatments. Procedia Engineering, 149: 346-351. https://doi.org/10.1016/j.proeng.2016.06.677

[7] Najwer, M., Niesłony, P. (2016). Evaluation of microhardness and strength properties of trimetal AA2519-AA1050-Ti6Al4V after various heat treatments (in Polish). Welding Technology Review, 88: 16-18. https://doi.org/10.26628/wtr.v88i4.589

[8] Boroński, D., Kotyk, M., Maćkowiak, P., Śnieżek, L. (2017). Mechanical properties of explosively welded AA2519-AA1050-Ti6Al4V layered material at ambient and cryogenic conditions. Materials & Design, 133: 390-403. https://doi.org/10.1016/j.matdes.2017.08.008

[9] Boroński, D., Kotyk, M., Maćkowiak, P. (2018). Crack initiation and growth analysis in explosively welded AA2519-AA1050-Ti6Al4V layered material in ambient and cryogenic conditions. Proceedings of the Institution of Mechanical Engineers, Part C: Journal of Mechanical Engineering Science, 232(8): 1470-1480. https://doi.org/10.1177/0954406217741516

[10] Boroński, D., Kotyk, M., Maćkowiak, P., Sołtysiak, R. (2018). Fatigue crack growth analysis in Al/Ti layered material in ambient and cryogenic conditions. Procedia Engineering, 213: 589-597. https://doi.org/10.1016/j.proeng.2018.02.054

[11] Bazarnik, P., Adamczyk-Cieślak, B., Gałka, A., Płonka, B., Snieżek, L., Cantoni, M., Lewandowska, M. (2016). Mechanical and microstructural characteristics of Ti6Al4V/AA2519 and Ti6Al4V/AA1050/AA2519 laminates manufactured by explosive welding. Materials & Design, 111: 146-157. https://doi.org/10.1016/j.matdes.2016.08.088

[12] Price, R.D., Jiang, F., Kulin, R.M., Vecchio, K.S. (2011). Effects of ductile phase volume fraction on the mechanical properties of Ti-Al3Ti metal-intermetallic laminate (MIL) composites. Materials Science and Engineering: A, 528(7-8): 3134-3146. https://doi.org/10.1016/j.msea.2010.12.087

[13] Romankov, S.E., Mukashev, B.N., Ermakov, E.L., Muhamedshina, D.N. (2004). Structural formation of aluminide phases on titanium substrate. Surface and Coatings Technology, 180-181: 280-285. https://doi.org/10.1016/j.surfcoat.2003.10.070

[14] Peruško, D., Petrović, S., Stojanović, M., Mitrić, M., Čizmović, M., Panjan, M., Milosavljević, M. (2012). Formation of intermetallics by ion implantation of multilatered Al/Ti nano-structures. Nuclear Instruments and Methods in Physics Research Section B: Beam Interactions with Materials and Atoms, 282: 4-7. https://doi.org/10.1016/j.nimb.2011.08.038

[15] Szachogluchowicz, I., Śnieżek, L., Torzewski, J., Grzelak, K. (2016). Fatigue cracking of AA2519-Ti6al4V laminate bonded by explosion welding. Solid State Phenomena, 250: 182-190. https://doi.org/10.4028/www.scientific.net/SSP.250.182

[16] Szachogluchowicz, I., Sniezek, L., Hutsaylyuk, V. (2015). Low cycle fatigue properties laminate AA2519-TI6AL4V. Procedia Engineering, 114: 26-33. https://doi.org/10.1016/j.proeng.2015.08.022

[17] Szachogluchowicz, I., Śnieżek, L., Hutsaylyuk, V. (2016). Low cycle fatigue properties of AA2519-Ti6Al4V laminate bonded by explosion welding. Engineering Failure Analysis, 69: 77-87. https://doi.org/10.1016/j.engfailanal.2016.01.001

[18] Raja, R., Jannet, S., Thampy, M.A. (2018). Synthesis and characterization of AA5083 and AA2024 reinforced with SiO_2 particles. Bulletin of the Polish Academy of Sciences: Technical Sciences, 66(2): 127-132. https://doi.org/10.24425/119066

[19] Kosturek, R., Lewczuk, R., Torzewski, J., Wachowski, M., Słabik, P., Maranda, A. (2023). Research on the post-weld explosive hardening of AA7075-T651 friction stir welded butt joints. Bulletin of the Polish Academy of Sciences: Technical Sciences, 71(4): 1-7. https://doi.org/10.24425/bpasts.2023.145685

[20] Milosavljević, M., Stojanović, N., Peruško, D., Timotijević, B., Toprek, D., Kovač, J., Dražič, G., Jeynes, C. (2012). Ion irradiation induced Al-Ti interaction in nano-scaled Al/Ti multilayers. Applied Surface Science, 258: 2043-2046. https://doi.org/10.1016/j.apsusc.2011.04.107

[21] Ma, M., Huo, P., Liu, W.C., Wang, G.J., Wang, D.M. (2015). Microstructure and mechanical properties of Al/Ti/Al laminated composites prepared by roll bonding. Materials Science and Engineering: A, 636: 301-310. https://doi.org/10.1016/j.msea.2015.03.086

[22] Luo, J.G., Acoff, V.L. (2004). Using cold roll bonding

and annealing to process Ti/Al multi-layered composites from elemental foils. Materials Science and Engineering: A, 379: 164-172. https://doi.org/10.1016/j.msea.2004.01.021
[23] Xia, H., Wang, S., Ben, H. (2014). Microstructure and mechanical properties of Ti/Al explosive cladding. Materials & Design (1980-2015), 56: 1014-1019. https://doi.org/10.1016/j.matdes.2013.12.012
[24] Kahraman, N., Gülenç, B., Findik, F. (2007). Corrosion and mechanical-microstructural aspects of dissimilar joints of Ti-6Al-4V and Al plates. International Journal of Impact Engineering, 34(8): 1423-1432. https://doi.org/10.1016/j.ijimpeng.2006.08.003
[25] Morizono, Y., Fukuyama, T., Matsuda, M., Tsurekawa, S. (2011). Solid- and liquid-solid reactions in aluminum-coated titanium substrate fabricated by using explosive energy. Materials Transactions, 52(12): 2178-2183. https://doi.org/10.2320/matertrans.M2011228
[26] Kotyk, M., Ziółkowski, W., Stachowiak, R., Swacha, P. (2021). The influence of cryogenic conditions on the critical crack tip opening displacement of titanium alloy Ti6Al4V (in Polish). Developments in Mechanical Engineering, 17(9): 18-31. https://doi.org/10.37660/dme.2021.17.9.2
[27] Kotyk, M., Strzelecki, P. (2024). Determination of the region of no effect of the notch on fatigue life of Aa2519 T62 aluminium alloy. Advances in Science and Technology Research Journal, 18(5): 156-174. https://doi.org/10.12913/22998624/190159
[28] Kotyk, M. (2020). Analysis of the fracture toughness of layered materials (in Polish). Bydgoszcz: Wydawnictwa Uczelniane Uniwersytetu Technologiczno-Przyrodniczego im. Jana i Jędrzeja Śniadeckich w Bydgoszczy.
[29] Walczuk-Gągała, P., Pater, Z., Wójcik, Ł. (2020). Determination of the value of the damage function in 1050A aluminium alloy. Advances in Science and Technology Research Journal, 14(2): 49-55. https://doi.org/10.12913/22998624/118105
[30] Zhang, W., Wang, M., Chen, W., Feng, Y., Yu, Y. (2016). Preparation of TiBw/Ti-6Al-4V composite with an inhomogeneous reinforced structure by a canned hot extrusion process. Journal of Alloys and Compounds, 669: 79-90. https://doi.org/10.1016/j.jallcom.2016.01.228
[31] ISO 4587:2003 Adhesives - Determination of tensile lap-shear strength of rigid-to-rigid bonded assemblies. Genewa: Standardization, International Organization. https://doi.org/10.3403/02844256

NOMENCLATURE

$\bar{x}$	average value of the measurement
x_i	value of a single measurement
n	number of measurements
P	represents area of the sheared surface
x	denotes length of sheared surface
y	indicates width of sheared surface
F	area of cut surface
τ	shear stresses
σ	standard deviation